

WHITECAP BUBBLES, BIG AND SMALL, AND THEIR ASYNCHRONOUS CONTRIBUTIONS TO SEA SALT AEROSOL PRODUCTION, AND SEA-AIR GAS TRANSFER

3.4

E.C. Monahan* & P. Vlahos
University of Connecticut at Avery Point, Groton, Connecticut

1. INTRODUCTION

It has long been recognized that the bursting of the bubbles produced in a breaking wave is the primary source of the sea-salt aerosol found in the marine atmosphere (e.g., Blanchard, 1963). The rate at which these bubbles reach the sea surface and burst is directly related to the rate of oceanic whitecap production, and the determination of the near-cubic dependence of whitecapping on wind speed, along with a recognition of the other factors that influence wave breaking, has made it possible to parameterize this marine aerosol production (e.g., Monahan, et al, 1986) for climate modeling, etc. (IPCC, 2001).

That the aggregation of bubbles in the bubble plumes beneath a whitecap also plays a major role in facilitating the air-sea transfer of gases such as CO₂, by forming a “low impedance vent” up to the immediate sea surface, was described some 25 years ago (Monahan and Spillane, 1984), and the near-cubic dependence of the gas transfer coefficient on wind speed for all but the calmest conditions, which follows from this physical model, has more recently gained widespread acceptance (e.g., Wanninkhof and McGillis, 1999).

2. SEQUENCE OF CONTRIBUTIONS

2.1 To Marine Aerosol Production

It has been shown, as is to be expected, that the large bubbles in the bubble plume beneath a whitecap, the major source of film

droplets, surface and break quickly, while smaller bubbles, the source of the jet droplets, take longer to rise to the sea surface and collapse (e.g., Woolf, et al, 1987).

2.2 To Sea-Air Gas Transfer

The role of the rapidly rising large bubbles, and the release of the buoyant potential energy associated with this action, in effectively stirring the immediate surface layer of the ocean right up through the “stagnant”, or laminar sub-layer, is easily seen to accommodate the sea-to-air, and air-to-sea, transfer of the wide range of gases found in our atmosphere and in solution in the sea, that are water-side controlled.

It is also recognized that the 50 µm-radius and larger bubbles, those that rise rapidly toward the sea surface and represent a disproportionate fraction of the aggregate bubble volume, can act as “gas elevators”, transporting gases that diffuse into the bubbles while submerged, to the sea surface and hence to the atmosphere. Likewise, atmospheric gases trapped in bubbles when they form as a wave breaks, are then transported to depth, and able to diffuse into the water column.

The bubble concentration in the plume beneath a whitecap decreases exponentially with depth, so the effect of the strong near-surface turbulence is to work against the vertical (upward) gradient in bubble concentration and this results in the net down-gradient (downward) transport of those much smaller bubbles whose buoyancy-associated vertical rise velocities are negligible. Small bubbles with surface-tension-induced overpressure, and relatively large surface-area to volume ratios, under most circumstances, rapidly dissolve. The fact that many of these smaller bubbles (certainly those of less than 10 µm-radius) entrained

Corresponding author address: Edward C. Monahan, Dept. of Marine Sciences, Univ. of Connecticut at Avery Point, Groton, CT 06340-6048; e-mail: ed.monahan@comcast.net

when a wave breaks never get back to the sea surface has implications for the effective transfer from water-to-air via the whitecap “vent” of certain gases of an amphiphilic nature. Any gas molecules that, even momentarily, adhere to the surface of these bubbles, and these are the bubbles with which most of the aggregate bubble surface area is associated, will contribute to a temporary reduction in the vertical gradient of dissolved gas concentration for a gas such as Dimethyl Sulfide, where the dissolved gas concentration typically exceeds the concentration in the overlying air. This will result in a net reduction in the effectiveness of the whitecap as a “low impedance vent”, and, as suggested by Vlahos and Monahan (2009), may explain the apparently anomalously low DMS transfer velocities, when compared with transfer velocities of other, non-amphiphilic gases, at the same wind speeds. It is to be noted that when these small bubbles dissolve, their surface load of DMS will be released back into the water column, and will help restore the prior gas concentration gradient, but by then the “low impedance vent” at the sea surface associated with the intensive large-bubble bursting event will long have disappeared, and the gas is again faced with the relatively ineffective mechanism of molecular diffusion to reach the immediate sea surface, the same situation it found itself in when there was no whitecap present.

It should also be noted that some of these very small bubbles never completely dissolve, but coated with a layer of surfactant organics (which often raft layer upon layer as these bubbles initially shrink while they are still losing gas to the surrounding sea water) such effectively neutrally buoyant bubbles with their now gas-impermeable coating persist as the “ghost bubbles” described by Johnson and Cooke (1981).

Vlahos and Monahan (2009) considered the total partial pressure of an amphiphilic molecule in seawater containing a significant number of non-rising bubbles with a total surface area due to bubbles per unit area of sea surface, Φ_B . A molecule with an affinity for this water-bubble boundary layer may experience a solubility enhancement that can be estimated using its octanol-water partition coefficient. The result is a change in the water-side fugacity of the compound at that instant. For compounds with a $Kow > 1$

(such as DMS for which $Kow = 6.3$) the effective Henry's Law constant can be predicted using; $H_{eff} = H / (1 + (C_{mix}/C_w) \Phi_B)$, where H is the dimensionless Henry's Law constant, C_{mix}/C_w is a dynamic solubility enhancement of the molecule due to bubbles and Φ_B is the fraction of bubble surface area per m^2 surface ocean. H_{eff} may be substituted in gas transfer models to predict the air-sea gas flux over a range of wind speeds for comparisons with field data.

3. BUBBLE PLUME EVOLUTION

Accurate measurements of the bubble spectrum just beneath an active spilling wave, i.e. within the α -plume beneath a Stage A Whitecap (see, e.g., Monahan and Lu, 1990, or Monahan, 2001), on the open ocean are still being sought, but detailed bubble measurements have been made within breakers in the surf zone (e.g., Deane, 1997). (Earlier measurements of bubble spectra just after the passage of a shallow water breaking wave are to be found in Blanchard and Woodcock (1957), and the near-surface bubble spectrum at an early stage in bubble plume decay has been inferred by Monahan (1988a) using the marine aerosol flux spectrum from the associated whitecap.)

At-sea bubble spectra that can be attributed to later stages in the dissolution of this bubble plume (i.e. attributable to the β -plume, the γ -plume, and the background bubble layer) can be assembled from the in situ measurements of Johnson and Cooke (1979), Kolovayev (1976), and others,

When the bubble spectrum (fig. 7) of Deane (1997), with a calibration correction as applied by Garrett et al (2000), is adopted as the spectrum of bubbles in an α -plume, it is apparent that this plume is rich in bubbles with radii at least as great as 3mm. (A likewise adjusted, simplified version of the original Deane (1997) spectrum is also to be found in Andreas and Monahan (2000), where its large-bubble-rich nature is likewise apparent.) If the spectrum 'B' of Monahan (1988b), which is based on the measurements of Johnson and Cooke (1979) and certain assumptions as to the geometry of the β -plumes found beneath Stage B whitecaps, is taken as a good representation of the bubble population in such a β -plume, and taking due account of the “across the board” reduction of bubble concentration due to the turbulent

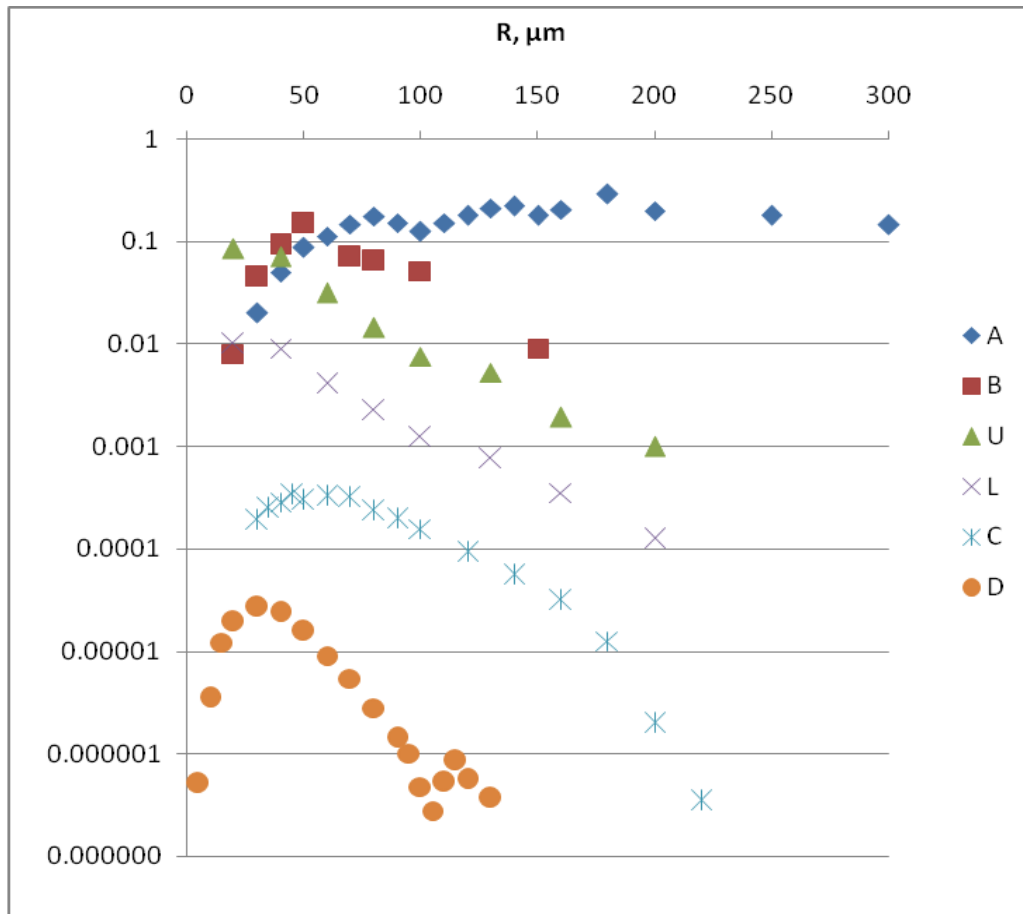


Figure 1. Plot of the aggregate surface area of air bubbles, per unit increment of bubble radius, per unit volume of sea water i.e. of $4 \pi R^2 \partial C/\partial R$, versus bubble radius, R . Each curve is meant to represent the differential aggregate surface area of air bubbles in the particular circumstance described below:

EXTENDED KEY TO FIGURE 1

A: This curve was derived from the $\partial C/\partial R$ vs R plot found in Figure 1 of Garrett et al (2000), and was based on Figure 7 of Deane (1997), which shows the bubble size spectrum in a breaking wave in the surf zone. Garrett et al (2000) had to correct an error that appeared in the original Deane (1997) plot due to a mis-assignment of radius values. An independently revised version of Deane's Figure 7, based on his power-law, i.e. straight-line, fits to his data the several size ranges, appears as Curve B' in Figure 1 of Andreas and Monahan (2000), and as Curve B in Figure 1 of Monahan

and Dam (2001). The present Curve A represents the aggregate surface area of the resident air bubbles, per increment of bubble radius, per unit volume of sea water just beneath a Stage A whitecap. (See Monahan and Lu (1990), particularly Figure 1, for the description of a Stage A whitecap.)

B: This curve is based on Curve B on the $\partial C/\partial R$ vs R plot that appears as Figure 1 of Monahan (1988b), and in turn was obtained by combining the coastal ocean bubble spectrum that appears on Figure 7 of Johnson and Cooke (1979) with some assumptions regarding the bubble plume geometry beneath a Stage B whitecap (see Monahan and Lu (1990) for definition of a Stage B whitecap.) The

current Curve B characterizes $4 \pi R^2 \partial C/\partial R$ vs R immediately beneath such a Stage B whitecap.

U and L: These two curves are the upper and lower limits on $4 \pi R^2 \partial C/\partial R$ in near-surface waters under a stage B whitecap respectively, based on the $\partial C/\partial R$ curves B_D and C_C found on Figure 2 of Monahan (1988b). Both curve B_D and curve C_C were obtained starting from an experimentally determined expression for the sea spray droplet flux from the surface of a Stage B whitecap (Equation 6 in Monahan et al, 1986), but with the application of different assumptions as to the rise velocity of the bubbles toward the surface of the whitecap, and as to the number of sea spray (jet) droplets produced when each bubble bursts. In the case of curve B_D it was assumed that the bubbles rose with the velocity of dirty bubbles (Thorpe, 1982), and that each bubble upon bursting produced one spray droplet. In the case of curve C_C it was assumed that each bubble had the rise velocity of a clean bubble (see, e.g. Figure 7.3 in Cliff et al, 1978), and that 5 droplets were injected upward into the air when it burst.

C: This curve is based on Figure 3, b (top, solid line) in Thorpe et al (2003), and represents $4 \pi R^2 \partial C/\partial R$ vs R at a depth of 2.1 meters beneath the surface in the downwelling bands (i.e., in the bubble curtains, marked Θ , beneath the windrows shown in Figure 1 of Monahan and Lu, 1990) produced when Langmuir cells are present in the oceanic surface layer.

D: This final curve is based on the $\partial C/\partial R$ vs R plot, showing the modeled steady-state mean bubble spectrum at a depth of 4 meters in the presence of Langmuir circulation and small-scale turbulence, when the ocean waters saturated with Nitrogen and Oxygen, that appears as the solid line in Figure 2 of Thorpe et al (1992).

3. PLUME EVOLUTION (Continued)

spreading of the bubble plume, then it remains clear that in the few seconds while

the α -plume decays into the β -plume, most of the very large ($> 200 \mu\text{m}$ radius) bubbles have risen, stirring the sea water right to the very surface. Once their buoyant energy has been dissipated, the “low impedance vent” facilitating gas exchange across the sea surface is essentially closed.

By contrast, if we look at the bubble spectrum measured by Thorpe, et al (2003) several meters below the sea surface in the downwelling bands of Langmuir circulations, i.e. in the bubble curtains (marked Θ) depicted on Fig. 1 of Monahan and Lu, 1990, we find that these old bubble populations are not only characterized by much lower bubble concentrations than are found in the α - and β -plumes, but are described by a spectrum that is quite narrow and has a peak at a bubble radius of about $50 \mu\text{m}$. The sharp falloff in this bubble spectrum as one moves to smaller radii is a reflection of the loss of most of the smaller bubbles due to dissolution. It is instructive to compare this spectrum with the mean steady-state bubble spectrum modeled by Thorpe et al (1992) to occur at a depth of 4 meters in the presence of Langmuir circulations, small-scale turbulence, and where the water is saturated with respect to nitrogen and oxygen. That the saturation levels in the ocean of the major gaseous constituents of the atmosphere have profound effects on the evolution of the sizes of individual bubbles has been demonstrated theoretically by Thorpe (1982), and experimentally by Stramska et al (1990).

The sequence whereby a bubble plume and the associated near surface concentration of bubbles evolve is consistent with the sequence in which first the large, and then the small, bubbles contribute to sea salt aerosol production, and to the phased roles of the various sized bubbles in the sea-to-air transfer of dissolved gases, including such amphiphilic species as DMS. Given the specific role ascribed in the Vlahos and Monahan (2009) model to the aggregate surface area of the submerged bubbles, particularly the small bubbles, in influencing the sea-air exchange of amphiphilic gases. Figure 1 is a plot showing the evolution with time of the aggregate bubble surface area spectrum, i.e., of $4 \pi R^2 \partial C/\partial R$, versus bubble radius, R.

4. CONCLUSIONS

The shortcomings of such simple physical conceptions of the role of whitecap bubbles in aerosol production, and in the air-sea exchange of gases, are acknowledged, though they do make explicit the localized, transient and asynchronous, nature of the processes that at all by the lowest wind speeds, control the air-sea flux of aerosols and gases.

5. RERERENCES

Andreas, E.L., and E.C. Monahan, 2000: The role of whitecap bubbles in air-sea heat and moisture exchange, *J. Phys. Oceanogr.*, **30**, 433-442.

Blanchard, D.C., 1963: The electrification of the atmosphere by particles from bubbles in the sea. *Prog. Oceanog.*, **1**, 71-202.

Blanchard, D.H., and A.H. Woodcock, 1957: Bubble formation and modification in the sea and its meteorological significance. *Tellus*, **9**, 145-158.

Cliff, R., J.R. Grace, and M.E. Weber. 1978. *Bubbles, Drops, and Particles*, Academic Press, New York.

Deane, G.B., 1997: Sound generation and air entrainment by breaking waves in the surf zone. *J. Acoust. Soc. Amer.*, **102**, 2671-2689.

Garrett, C., M. Li, and D. Farmer, 2000: The connection between bubble size spectra and energy dissipation rates in the upper ocean. *J. Phys. Oceanogr.*, **30**, 2163-2171.

IPCC, 2001: *Climate Change 2001: The Scientific Basis, Contributions of Working Group I to the Third Assessment Report*, UNEP, WMO.

Johnson, B.D., and R.C. Cooke, 1979: Bubble populations and spectra in coastal waters: A photographic approach. *J. Geophys. Res.* **84**, 3761-3766.

Johnson, B.D., and R.C. Cooke, 1981: Generation of stabilized microbubbles in seawater. *Science*, **213**, 209-211.

Kolovayev, P.A., 1976: Investigation of the concentration and statistical size distribution of wind-produced bubbles in the near-surface ocean layer. *Oceanology*, **15**, 659-661.

Monahan, E.C., 1988a: Whitecap coverage as a remotely monitorable indication of the rate of bubble injection into the oceanic mixed layer, in *Sea Surface Sound*, B.R. Kerman, ed., Kluwer Academic, 85-96.

Monahan, E.C., 1988b: Near-surface bubble concentration and oceanic whitecap coverage. *Preprint Vol., 7th Conf. on Ocean-Atmos. Interact., Anaheim*, Am. Met. Soc., 178-181.

Monahan, E.C., 2001: Air-sea interaction: Whitecaps and foam, in *Encyclopedia of Ocean Sciences*, J. Steele, S. Thorpe, and K. Turekian, eds., Academic Press, 3213-3219.

Monahan, E.C., and H.G. Dam. 2001. Bubbles: An estimate of their role in the global flux of carbon, *Journal of Geophysical Research*, **106**, pp. 9377-9383.

Monahan, E.C., and M. Lu, 1990: Acoustically relevant bubble assemblages and their dependence on meteorological parameters. *IEEE J. of Oceanic Eng.* **15**, 340-349.

Monahan, E.C., D.E. Spiel, and K.L. Davidson, 1986: A model of marine aerosol production via whitecaps and wave disruption, in *Oceanic Whitecaps, and Their Role in Air-Sea Exchange Processes*, E.C. Monahan and G. MacNiocaill, eds., D. Reidel Pub., 167-174.

Monahan, E.C., and M.S. Spillane, 1984: The role of oceanic whitecaps in air-sea gas exchange, in *Gas Transfer at Water Surfaces*, W. Brutsaert and G.J. Jirka, eds., D. Reidel Pub., 495-503.

Stramska, M., R. Marks, and E.C. Monahan, 1990: Bubble-mediated aerosol production

as a consequence of wave breaking in supersaturated (hyperoxic) seawater. *J. Geophys. Res.*, **95**, 18281-18288.

Thorpe, S.A., 1982: On the clouds of bubbles formed by breaking wind-waves in deep water, and their role in air-sea gas transfer. *Philos. Trans. R. Soc., London, Ser. A*, **304**, 155-210.

Thorpe, S.A., P. Bowyer, and D.K. Woolf, 1992: Some factors affecting the size distributions of oceanic bubbles. *J. Phys. Oceanogr.* **22**, 382-389.

Thorpe, S.A., T.R. Osborn, D.M. Farmer, and S. Vagle, 2003: Bubble clouds and Langmuir circulation: Observations and models. *J. Phys. Oceanogr.* **33**, 2013-2031.

Vlahos, P., and E.C. Monahan, 2009: A generalized model for the air-sea transfer of dimethyl sulfide at high wind speeds. *Geophys. Res. Lett.*, **36**, L21605.

Wanninkhof, R., and W.R. McGillis, 1999: A cubic relationship between air-sea CO₂ exchange and wind speed. *Geophys. Res. Lett.*, **26**, 1889-1892.

Wolf, D.K., P.A. Bowyer, and E.C. Monahan, 1987: Discriminating between the film-drops and the jet-drops produced by a simulated whitecap. *J. Geophys. Res.* **92**, 5142-5150.